Доклади на Българската академия на науките
Comptes rendus de l'Académie bulgare des Sciences
Tome 79, No 8, 2026

GEOPHYSICS
Meteorology

STATISTICAL ASSESSMENT OF THE INFLUENCE OF SAHARAN DUST ON DIRECT SOLAR RADIATION IN BULGARIA

Vanya D. Maneva[1]✉, **Anton B. Petrov**[2]

Received on May 20, 2026
Presented by K. Stoykova, Corresponding Member of BAS, on July 28, 2026

Abstract

Mineral dust can attenuate surface direct solar radiation, but its statistical signature is often difficult to isolate from the much stronger influence of cloud cover. This study provides a statistical assessment of the influence of Saharan dust on direct solar radiation in Bulgaria during the period 1 July 2020–30 June 2025. The analysis combines daily pyranometer observations from Sofia, Sandanski and Ahtopol with satellite-derived dust aerosol optical depth at 550 nm ($DAOD_{550}$) and ERA5 total cloud cover. Direct solar radiation was normalized by daily extraterrestrial radiation on a horizontal surface in order to reduce the influence of solar geometry and day length. A sequence of five linear regression models was used to test the robustness of the estimated dust effect under progressively stricter controls for cloud cover, station-related differences and residual seasonality. In the principal full-sample model, $DAOD_{550}$ retained a statistically significant negative coefficient ($\beta = -0.0804$, $p = 0.002$), while in the nearly clear-sky subset the effect became stronger ($\beta = -0.1935$, $p < 0.001$). The obtained results suggest that Saharan dust transport is associated with a measurable attenuation of direct solar radiation at the surface over Bulgaria, with the dust-related signal becoming more clearly detectable when cloud influence is reduced.

Key words: Saharan dust, DAOD, direct solar radiation

Introduction. Solar radiation is a key component of the atmospheric energy balance and an important factor in climate studies and solar energy applications.

https://doi.org/10.7546/CRABS.2026.08.07

During its passage through the atmosphere, direct solar radiation is attenuated by scattering and absorption caused by clouds and atmospheric particles [1–3]. Among atmospheric aerosols, mineral dust transported from desert regions is one of the natural factors with strong potential to modify radiative transfer, particularly the direct solar radiation reaching the surface [2, 3].

Saharan dust outbreaks frequently affect southeastern Europe and the Balkan Peninsula, including Bulgaria [4, 5]. Such events are associated with increased atmospheric turbidity and may lead to a measurable attenuation of direct solar radiation at the surface. However, the quantitative separation of the dust effect from the much stronger influence of cloud cover remains a major difficulty in observational analyses.

This difficulty is especially important in regional studies based on ground observations combined with gridded satellite and reanalysis products. In such settings, the statistical signal of dust must be interpreted against a background of strong cloud-related variability, local station differences and residual seasonal structure. Therefore, the problem is not merely whether dust affects direct radiation in principle, but whether that effect can be detected consistently after the dominant confounding influences are taken into account.

The objective of the present study is to assess statistically the relationship between Saharan dust loading, represented by dust aerosol optical depth at 550 nm ($DAOD_{550}$), and direct solar radiation in Bulgaria. For this purpose, daily pyranometer observations from three stations were combined with satellite-derived $DAOD_{550}$ and ERA5 total cloud cover data for the period 1 July 2020–30 June 2025. A sequence of regression models was applied in order to evaluate the robustness of the estimated dust effect under different levels of statistical control.

Data and methods. ***Study area and datasets.*** This study covers the period from 1 July 2020 to 30 June 2025 and includes three stations in Bulgaria: Sofia (42.653835°N, 23.382884°E), Sandanski (41.55°N, 23.2672°E), and Ahtopol (42.0839°N, 27.9522°E). Direct solar radiation and sunshine duration were obtained from pyranometer observations at the respective stations (Fig. 1).

Dust aerosol optical depth at 550 nm ($DAOD_{550}$) was obtained from the Copernicus Climate Data Store dataset *Aerosol properties gridded data from 1995 to present derived from satellite observations* [6]. In the study period, the variability of $DAOD_{550}$ was interpreted as being dominated primarily by episodes of Saharan dust transport and was therefore used as an indicator of dust loading in the atmosphere.

It should be emphasized that the Copernicus product used here provides dust aerosol optical depth rather than total aerosol optical depth. For this reason, the analyzed variability is interpreted primarily as variability in mineral dust loading. Over Bulgaria, such variability is expected to be dominated mainly by transported Saharan dust episodes, while other aerosol sources such as urban pollution, biomass burning and sea salt are likely to contribute comparatively less

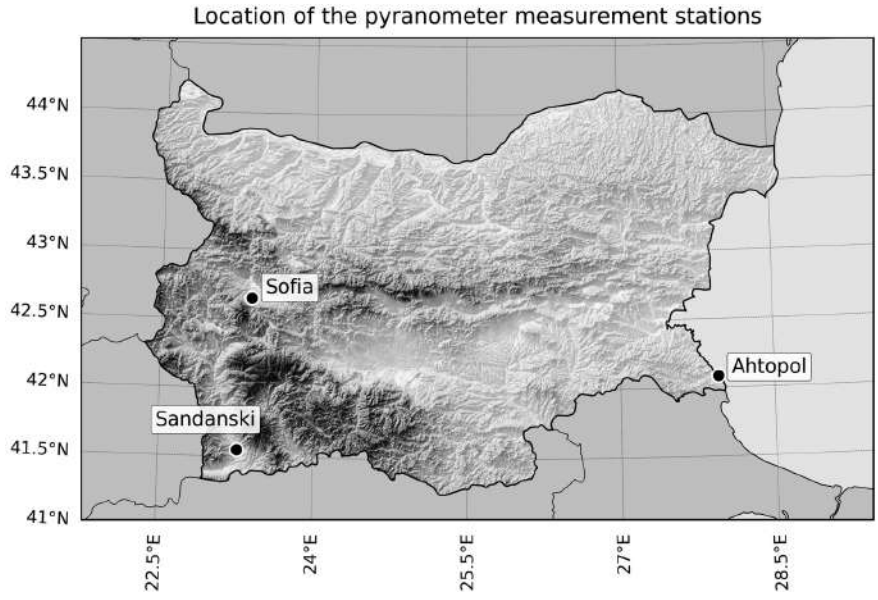


Fig. 1. Location of the study stations in Bulgaria

to the dust-specific optical depth field.

Total cloud cover (TCC) was obtained from the Copernicus Climate Data Store dataset *ERA5 hourly data on single levels from 1940 to present* [7, 8]. For each station, both $DAOD_{550}$ and TCC values were assigned from the grid cell containing the station location.

Data processing and normalization. The station observations, satellite-derived $DAOD_{550}$ and ERA5 cloud cover data were merged into a common daily dataset by date and station. Hourly ERA5 cloud cover values were aggregated into a daylight mean cloud cover metric.

Direct solar radiation was normalized by daily extraterrestrial radiation on a horizontal surface in order to reduce the influence of solar geometry and day length:

$$R_{\text{norm}} = \frac{R_{\text{dir}}}{R_{0h}}, \tag{1}$$

where R_{norm} is the normalized direct solar radiation (-), R_{dir} is the measured daily direct solar radiation sum (MJ m^{-2} day^{-1}), and R_{0h} is the daily extraterrestrial radiation on a horizontal surface (MJ m^{-2} day^{-1}). The latter was calculated following standard solar geometry relations [9] as

$$R_{0h} = \frac{24 \cdot 3600}{\pi} G_{sc} d_r \left[\omega_s \sin\phi \sin\delta + \cos\phi \cos\delta \sin\omega_s\right], \tag{2}$$

where G_{sc} is the solar constant (W m^{-2}), d_r is the inverse relative Earth–Sun

distance factor (-), ϕ is latitude (rad), δ is solar declination (rad), and ω_s is the sunset hour angle (rad).

Statistical models. This study applied linear regression models estimated by ordinary least squares (OLS), with heteroskedasticity-robust standard errors of type HC3 [10, 11]. Residual seasonality was represented by harmonic terms based on the day of the year (J):

$$S_1 = \sin\left(\frac{2\pi\, J}{365.25}\right), \quad S_2 = \cos\left(\frac{2\pi\, J}{365.25}\right). \tag{3}$$

A sequence of five model specifications was examined in order to test the stability of the estimated dust effect under progressively stricter controls for cloud cover, station-related differences and residual seasonality:

- Model 1: $R_{\text{norm}} \sim DAOD_{550}$
- Model 2: $R_{\text{norm}} \sim DAOD_{550} + TCC$
- Model 3: $R_{\text{norm}} \sim DAOD_{550} + TCC + station + S_1 + S_2$
- Model 4: $R_{\text{norm}} \sim DAOD_{550} + TCC + DAOD_{550} \times TCC + station + S_1 + S_2$
- Model 5: Model 3 applied to the nearly clear-sky subset defined by $TCC \leq 0.20$

The threshold $TCC \leq 0.20$ was selected as a pragmatic criterion for nearly clear-sky conditions, with the aim of substantially reducing cloud influence while preserving a sufficient sample for regression analysis. The selected value therefore represents a compromise between physical interpretability and statistical robustness. This reasoning is consistent with previous clear-sky identification studies, where somewhat higher cloud-fraction thresholds (e.g., 25%) were also adopted in order to avoid excessive loss of data while still limiting cloud contamination [12].

Station fixed effects were included to account for persistent site-specific differences not explicitly represented by the other predictors. The estimated coefficients of the five models are summarized in Table 1.

Results and discussion. A positive but nonlinear relationship was found between daily direct solar radiation sum and sunshine duration at the three study stations (Fig. 2). The LOWESS-smoothed curves indicate a change in curvature at sunshine duration values of approximately 7 h, suggesting that the increase in direct solar radiation is not uniform across the full range of sunshine duration. This behaviour is physically consistent with the combined effects of solar geometry, cloud conditions and atmospheric transparency.

At the same time, the raw relationship between $DAOD_{550}$ and normalized direct solar radiation appears visually weak in simple scatterplots. This is expected,

Table 1

Estimated coefficients of the five regression models relating normalized direct solar radiation to $DAOD_{550}$, cloud cover and additional controls. Robust HC3 standard errors are shown in parentheses

	Model 1	Model 2	Model 3	Model 4	Model 5
Constant	0.6604^{***}	0.7458^{***}	0.7355^{***}	0.7478^{***}	0.7180^{***}
	(0.003)	(0.003)	(0.004)	(0.004)	(0.004)
$DAOD_{550}$	-0.1129^{***}	-0.0365	-0.0804^{**}	-0.2330^{***}	-0.1935^{***}
	(0.027)	(0.023)	(0.026)	(0.035)	(0.036)
95% CI ($DAOD_{550}$)	[−0.166, −0.060]	[−0.082, 0.009]	[−0.132, −0.029]	[−0.301, −0.165]	[−0.265, −0.122]
TCC	—	-0.2926^{***}	-0.2933^{***}	-0.3249^{***}	—
	—	(0.009)	(0.009)	(0.012)	—
$DAOD_{550}$ × TCC	—	—	—	0.3815^{***}	—
	—	—	—	(0.084)	—
$\sin(J)$	—	—	0.0164^{***}	0.0164^{***}	0.0185^{***}
	—	—	(0.003)	(0.003)	(0.002)
$\cos(J)$	—	—	-0.0201^{***}	-0.0206^{***}	-0.0183^{***}
	—	—	(0.003)	(0.003)	(0.003)
Station fixed effects	No	No	Yes	Yes	Yes
Seasonal harmonic terms	No	No	Yes	Yes	Yes
R^2	0.004	0.337	0.364	0.366	0.117
n	2944	2944	2944	2944	1118

$^{**}p < 0.01$, $^{***}p < 0.001$. Model 5 is estimated for the nearly clear-sky subset defined by $TCC \leq 0.20$.

since the dust signal is superimposed on stronger sources of variability, most notably cloud cover, as well as station-related differences and residual seasonality. For this reason, the effect of Saharan dust was evaluated through a sequence of regression models with progressively stricter controls.

The results of the five models are summarized in Table 1. In the simplest specification (Model 1), $DAOD_{550}$ already shows a negative association with normalized direct solar radiation. After inclusion of cloud cover in Model 2, the estimated dust effect remains negative, while cloud cover emerges as the dominant explanatory factor. In Model 3, which additionally includes station fixed effects and harmonic seasonal terms, the coefficient of $DAOD_{550}$ remains negative and statistically significant, indicating that the dust effect persists after adjustment for the main confounding influences. Model 4 further tests the interaction between $DAOD_{550}$ and cloud cover and is intended to examine whether the estimated dust effect changes under different cloud conditions.

The positive interaction coefficient in Model 4 suggests that the negative association between $DAOD_{550}$ and normalized direct solar radiation becomes weaker

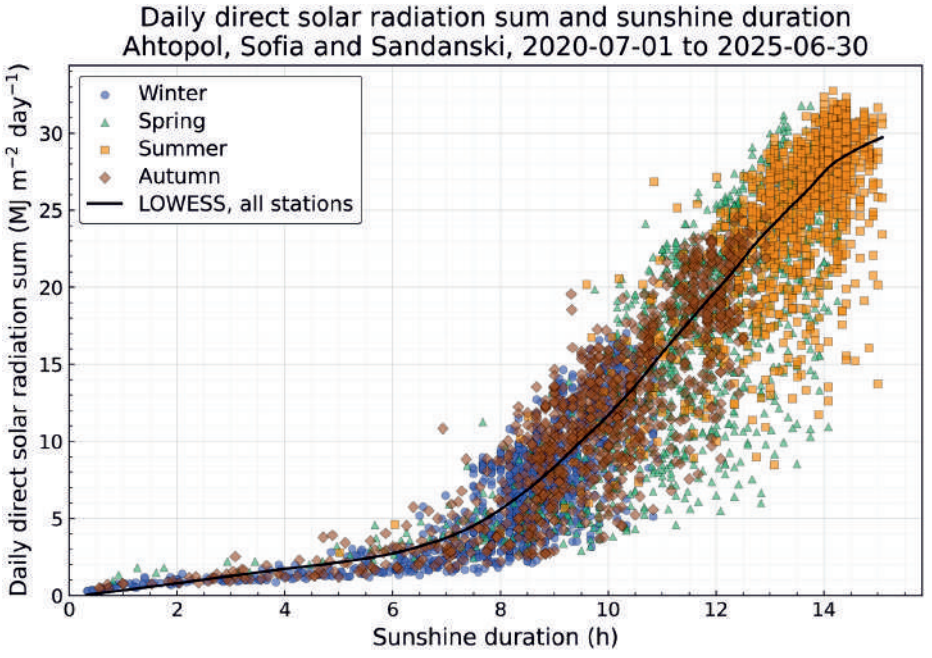


Fig. 2. Scatterplots showing the relationship between daily direct solar radiation sum (MJ m^{-2} day^{-1}) and sunshine duration (h) at Ahtopol, Sofia and Sandanski during the period 1 July 2020–30 June 2025. The black curve represents LOWESS smoothing ($frac = 0.25$)

as cloud cover increases. This is physically plausible, since under increasingly cloudy conditions the attenuation by clouds dominates the radiation regime and may partially mask the dust-related signal. In the present study, Model 4 is interpreted primarily as an exploratory robustness specification rather than as the principal model.

The clearest result is obtained for Model 5, estimated for the nearly clear-sky subset ($TCC \leq 0.20$). In this case, the coefficient of $DAOD_{550}$ becomes more negative than in the full-sample multivariate model, indicating that part of the dust signal in the complete dataset is masked by cloud variability. This tendency is also evident in the binned nearly clear-sky relationship shown in Fig. 3, where normalized direct solar radiation decreases with increasing dust loading.

Taken together, the sequence of models provides a consistent picture. Cloud cover is the dominant control on normalized direct solar radiation in the full dataset, but $DAOD_{550}$ retains a statistically significant negative effect after adjustment for cloudiness, station-related differences and residual seasonality. Under nearly clear-sky conditions, this negative effect becomes stronger, supporting the interpretation that Saharan dust contributes independently to the attenuation of direct solar radiation at the surface over Bulgaria.

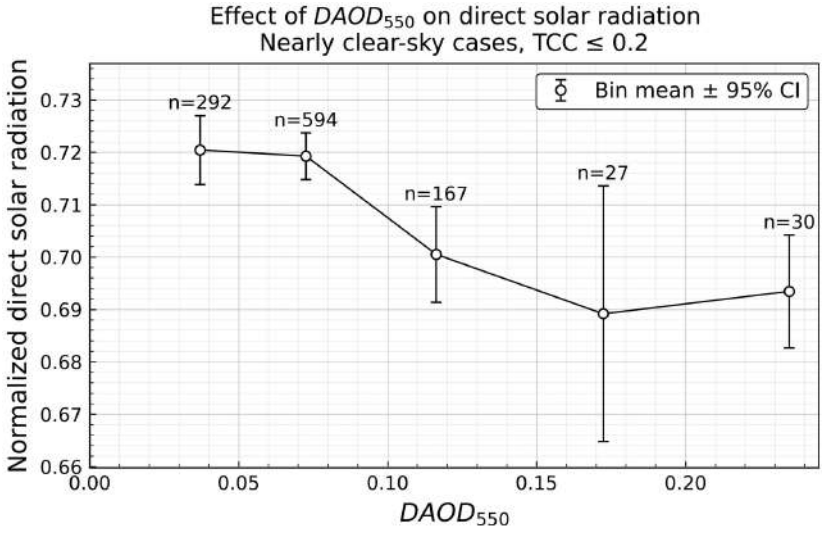


Fig. 3. Binned relationship between $DAOD_{550}$ and normalized direct solar radiation under nearly clear-sky conditions ($TCC \leq 0.20$). Points represent mean values of normalized direct solar radiation within predefined $DAOD_{550}$ intervals, and vertical bars denote 95% confidence intervals

Conclusions. This study provides statistical evidence that Saharan dust transport is associated with a measurable attenuation of direct solar radiation at the surface in Bulgaria. The sequence of regression models shows that the estimated dust effect remains negative after accounting for cloud cover, station-related differences and residual seasonality. The strongest negative coefficient of $DAOD_{550}$ is obtained for the nearly clear-sky subset, indicating that cloud variability partly masks the dust-related signal in the full dataset.

At the same time, the results should be interpreted with appropriate caution, since the analysis is observational and the aerosol and cloud variables are derived from gridded products rather than strictly local measurements. Therefore, the reported relationships are best understood as statistically robust associations rather than as direct proof of causality.

Overall, the results support the interpretation that Saharan dust transport contributes independently to attenuation of surface direct solar radiation over Bulgaria, with the signal becoming more clearly detectable when cloud influence is reduced. Further work may include a more detailed analysis of interaction effects, nonlinear responses and seasonal stratification.

Acknowledgements. The authors would like to express their sincere gratitude to the Bulgarian Academy of Sciences (BAS) for providing the opportunity to present and publish the results of this study. They also gratefully acknowledge the colleagues at the National Institute of Meteorology and Hydrology (NIMH) whose support, assistance and professional guidance contributed to the realization of this work.

REFERENCES

[1] IPCC (2023) Climate Change 2023: Synthesis Report. Contribution of Working Groups I, II and III to the Sixth Assessment Report of the Intergovernmental Panel on Climate Change, Geneva, IPCC.

[2] Yu H., Y. J. Kaufman, M. Chin et al. (2006) A review of measurement-based assessments of the aerosol direct radiative effect and forcing, Atmos. Chem. Phys., **6**, 613–666.

[3] Kok J. F., T. Storelvmo, V. A. Karydis et al. (2023) Mineral dust aerosol impacts on global climate and climate change, Nat. Rev. Earth Environ., **4**, 71–86.

[4] Ilieva R., K. Stoev, G. Guerova (2025) Climatology and circulation classification of Saharan dust over Bulgaria, J. Atmos. Sol.-Terr. Phys., **267**, 106403.

[5] Peshev Z., A. Deleva, L. Vulkova, T. Dreischuh (2022) Large-scale Saharan dust episode in April 2019: Study of desert aerosol loads over Sofia, Bulgaria, using remote sensing, in situ, and modeling resources, Atmosphere, **13**, 981.

[6] Copernicus Climate Change Service, Climate Data Store (2019) Aerosol properties gridded data from 1995 to present derived from satellite observations.

[7] Copernicus Climate Change Service, Climate Data Store (2018) ERA5 hourly data on single levels from 1940 to present.

[8] Hersbach H., B. Bell, P. Berrisford et al. (2020) The ERA5 global reanalysis, Q. J. R. Meteorol. Soc., **146**, 1999–2049.

[9] Allen R. G., L. S. Pereira, D. Raes, M. Smith (1998) Crop evapotranspiration: Guidelines for computing crop water requirements, FAO Irrigation and Drainage Paper 56, Rome, FAO.

[10] White H. (1980) A heteroskedasticity-consistent covariance matrix estimator and a direct test for heteroskedasticity, Econometrica, **48**(4), 817–838.

[11] MacKinnon J. G., H. White (1985) Some heteroskedasticity-consistent covariance matrix estimators with improved finite sample properties, J. Econometrics, **29**(3), 305–325.

[12] Correa F., R. Escobar, R. Galleguillos et al. (2022) A method for clear-sky identification and long-term trends assessment using daily surface solar radiation records, Earth Space Sci., **9**, e2021EA002197.

[1]*National Institute of Meteorology and Hydrology,*
66 Tsarigradsko Shosse, 1784 Sofia, Bulgaria
e-mail: vanya.maneva@meteo.bg (https://orcid.org/0009-0001-1717-036X)

[2]*BULATSA, 1 Brussels Blvd, 1540 Sofia, Bulgaria*
e-mail: anton.botev.petrov@gmail.com (https://orcid.org/0000-0003-0853-6347)